ACS OMEGA

Open Access

http://pubs.acs.org/journal/acsodf

Article

Effects of Alkali Activation of the Cotton Straw Biochar on the Adsorption Performance for Cd^{2+}

Nuremanguli Tuersun, Yingjie Wang, Aikelaimu Aihemaiti, Jing Wang,* and Chuanjing Huang

Cite This: *ACS Omega* 2024, 9, 17989−18000

Read Online

ACCESS | Metrics & More | Article Recommendations

ABSTRACT: In this study, a single factor exploration method was adopted to optimize the cotton shell-based activated carbon adsorption reaction time, temperature, pH value, initial concentration of cadmium ion, and other conditions. The experimental results showed that under the conditions of Cd^{2+} solution pH = 8, initial concentration of 100 mg/L, adsorption reaction time of 180 min, adsorption temperature of 45 °C, cotton shell-based activated carbon dosage of about 0.1 g, the removal rate of Cd^{2+} was 94.03%, the adsorption capacity was 51.95 mg/g, and the error was only 0.05%. The adsorption kinetic analysis of this study conforms to the quasi-second-order kinetic model, the adsorption isotherm analysis conforms to the Langmuir adsorption isothermal model, and the Gibbs free energy of the adsorption process is negative; the above simulation analysis also proves the spontaneity and feasibility of the adsorption process.

1. INTRODUCTION

Activated carbon is an excellent microcrystalline carbon material with a large specific surface area, developed pore structure, unique adsorption ability, and good stability at high temperatures. There are a large number of invisible micropores in activated carbon materials, and the surface area of 1 g of activated carbon can reach up to 800−1500 m^2.[1−3,7] The adsorption mechanism is mainly based on the intermolecular adsorption force (the van der Waals force) for adsorption. Some modified activated carbon exhibits both physical and chemical adsorption during the adsorption process, although the molecular motion speed is affected by temperature and material; however, it always undergoes irregular movements in the microenvironment. When a molecule is captured by the pores of activated carbon and enters the pores due to mutual attraction between molecules, more molecules are continuously attracted until they fill the pores of activated carbon.[5]

At present, the main raw materials used for the commercial production of activated carbon are materials with high carbon content, such as petroleum residues.[1] However, these materials are expensive and nonrenewable and can also cause serious environmental pollution. In order to deepen the prevention and control of environmental pollution and meet the requirements of sustainable development of the environment, the study of clean materials to replace traditional materials to prepare activated carbon has become one of the current research hotspots. Biomass materials with high yield, low cost, high carbon content, and renewable energy fully meet the requirements.[2,24,26,29] At present, the biomass raw materials used for the preparation of activated carbon include various fruit and wood husks (such as peanut husks, rice husks, etc.), cotton straw, wheat straw, corn straw, sugar cane bagasse, bamboo, and so forth.

As is well known, cotton is one of the most important and widely planted crops in the world. China, India, and the United States rank among the top three cotton producers in the world. As the world's top cotton-producing country, China's annual production in 2022/2023 is about 6.684 million tons, accounting for 26% of the world's total cotton production. India's cotton production is relatively close to China's, accounting for 22% of the world's annual production in 2022/2023. The US cotton production in the same year accounted for 12.3% of the global total (data source: USDA). Cotton cultivation in China is mainly concentrated in the Xinjiang Autonomous Region, the Yangtze River Basin, and the Huanghuai region. Xinjiang has long been the main cotton-producing area in China. In the process of promoting the development of the Chinese path to modernization, Xinjiang's cotton planting area continues to expand while its cotton yield per unit area also continues to increase, which plays a positive role in developing the local economy and increasing farmers' income. At present, the cotton planting area in Xinjiang exceeds

Received: November 28, 2023
Revised: March 28, 2024
Accepted: March 29, 2024
Published: April 12, 2024

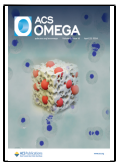

2.5 million ha and the annual production of cotton straw exceeds 20 million tons (data from the China National Knowledge Infrastructure). If a large amount of straw is randomly stacked or burned, it not only wastes resources but also causes environmental pollution. If the cotton straw biomass resources in southern Xinjiang can be fully and reasonably utilized and the technology of cotton straw resource recycling and utilization can be promoted, it can not only solve the problems of energy scarcity and uneven distribution but also reduce environmental loads, increase farmers' economic benefits, meet the requirements of green and low-carbon development, and have broad development prospects and significance in preventing energy loss and developing green environmental protection benefits.

Cadmium pollution in water bodies mainly comes from surface runoff and industrial wastewater, with pollution second only to mercury and lead. The more mature treatment technology in sewage treatment is the adsorption method,[3,7] which is characterized by high efficiency and environmental protection. This study takes cotton shell-based activated carbon as the research object to explore its adsorption performance for Cd^{2+} simulated wastewater, providing a theoretical basis for the preparation and application of cotton straw-based biochar and improving the level of crop straw resource utilization.

2. MATERIALS AND METHODS

In this experiment, cotton straw was taken from Yingjisha, Xinjiang, China, as the research object, as shown in Figure 1 and

Figure 1. Cotton stem.

Figure 2 ("Photograph courtesy of "Yingjie Wang". Copyright 2024"). Cotton stems and cottonseed hulls were, respectively, activated by a single KOH and KOH/NaOH composites, and $KMnO_4$ was used for the preoxidation treatment and prepared into activated carbon. The prepared activated carbon was characterized and analyzed by low-temperature N_2 adsorption, BET, and Langmuir theory, and the influence of the preoxidation treatment on the surface pore structure and surface characteristics of activated carbon was investigated.

2.1. Materials. Nitrogen (99.99%, Xinjiang China Keyuan Gas Manufacturing Co., Ltd.), distilled water (primary water), sodium hydroxide (analytically pure), potassium hydroxide (analytically pure), potassium permanganate (analytically pure), hydrochloric acid (analytically pure), nitric acid (analytically pure), cadmium nitrate (analytically pure), and all chemical reagents were purchased from Tianjin China Zhiyuan Chemical Reagent Co., Ltd.

Figure 2. Cotton shell.

2.2. Instruments. Multifunctional crusher (600A), electronic balance (JEA2002), open-tube electric furnace (T2100A), constant-temperature drying oven (240A), electrothermal water bath (DZKW-S-4), scanning electron microscope (Nova NanoSEM 450), infrared spectrometer (IS50), inductively coupled ion mass spectrometer (ICP-MS EXPEC7000), flame atomic absorption mass spectrometer (WFX-220A Es), specific surface area, and pore size analyzer (BET-ASAP2460) were used.

2.3. Preparation of the Cotton Straw Biochar.

2.3.1. Experimental Methods. 2.3.1.1. Carbonization Treatment.

1 The cotton stalk and cotton shell were soaked and cleaned with distilled water to remove the impurities on their surface, and then placed in a drying oven and dried at 378 K for 12 h. The dried sample was taken out, crushed into powder with a crusher, sieved with a 0.45 mm sieve, and then a certain amount of powder was loaded into a sealed bag and dried in the drying oven for 24 h.
2 About 100 g of cotton straw powder was placed into the quartz boat striping with N_2 for 20 min to remove other gases in the pipe. The flow rate of the tubular furnace was set at 0.15 L/min, the heating rate was 10 K/min, and the carbonization temperature was 573 K. After the temperature reached 573 K, carbonization was done at this temperature for 30 min. Then, the temperature was allowed to cool to 313 K, and the carbonized product was taken out safely.

2.3.1.2. Activation Treatment.

1 About 100 g of the carbonized material, 100 mL of the single activator KOH (0.1 mol/L), and 100 mL of the composite activator KOH/NaOH (0.1 mol/L) were weighed, and the carbonized material was impregnated with a carbon−nitrogen ratio of 1:2.[3,34−36] It was mixed evenly, kept in a water bath at 353 K for 18 h, and then placed into a drying oven at 378 K for 24 h.
2 The dried filter residue was placed in the tubular resistance furnace, respectively, and activated for 40 min when the temperature was heated to 973 K. It was allowed to cool down to room temperature and the activated products were safely removed.
3 The product was impregnated with dilute hydrochloric acid (0.1 mol/L) and then repeatedly rinsed with 353 K distilled water until the solution pH was neutral. The solution was filtered, leaving the filter residue, and placed

https://doi.org/10.1021/acsomega.3c09501
ACS Omega 2024, 9, 17989−18000

in the blast box to dry for about 12 h until a constant weight was achieved. The dried filter residue was taken out, smashed, and passed through a 200 mesh sieve to obtain powdered cotton stalk and cottonseed hull activated carbon, as shown in Figure 3 and Figure 4

Figure 3. Cotton stem-based activated carbon.

Figure 4. Cotton shell-based activated carbon.

("Photograph courtesy of "Yingjie Wang". Copyright 2024").

2.3.1.3. Preoxidation Treatment. In order to increase the porosity and specific surface area of activated carbon, cotton shell-based activated carbon was preoxidized with $KMnO_4$ (0.1 mol/L). First, the samples activated by different activators were impregnated with 100 mL of the $KMnO_4$ oxidant (0.1 mol/L) in the ratio of 1:4, stirred evenly, soaked in a 353 K water bath for 5 h, then soaked at room temperature for 18 h, then filtered and dried in a constant-temperature blast drying oven (378 K drying for 24 h), and the dried samples were retained for standby.

2.4. Preparation of Simulated Wastewater Containing Cd^{2+}. 2.7440 g of $Cd(NO_3)_2{\cdot}4H_2O$ was accurately weighed and 1 mg/mL of the Cd^{2+}standard stock solution was prepared with 0.2% nitric acid to 1000 mL. Then, according to the experimental needs, 20, 40, 60, 80, 100, and 120 mL of the standard stock solution were converted to 1000 mL to prepare simulated wastewater containing Cd^{2+} at concentrations of 20, 40, 60, 80, 100, and 120 mg/L.

2.5. Static Adsorption Experiment. About 1 g of cotton straw-modified biomass activated carbon was weighed, added to 100 mL of Cd^{2+}solution with different concentrations, and placed it in a constant-temperature oscillator for adsorption reaction at a certain temperature. After adsorption, the concentration of Cd^{2+} before and after adsorption was measured using a flame atomic absorption spectrophotometer,[3,21,27,28,30] and the removal rate p and adsorption capacity q_t of Cd^{2+} by cotton straw-modified biomass activated carbon were calculated according to formula 1 and 2.

The calculation formula for the removal rate (%) is

$$p = \frac{C_0 - C_t}{C_0} \times 100\% \quad (1)$$

The adsorption capacity q_t (mg·g^{-1}) formula is

$$q_t = \frac{V(C_0 - C_t)}{m} \quad (2)$$

In the formula, C_0 is the initial concentration of metal Cd^{2+}(mg/L), C_t is the concentration of metal Cd^{2+} after adsorption (mg/L), t is the adsorption time (min), and m is the mass of the adsorbent (g).

3. RESULTS AND DISCUSSION

3.1. Characterization. *3.1.1. BET Characterization.* To facilitate the comparative study, the cotton stem-based activated carbon (KOH/NaOH activated), cotton stem-based activated carbon (KOH activated), preoxidized cotton stem-based activated carbon (KOH/NaOH activated), preoxidized cotton stem-based activated carbon (KOH activated), cotton husk-based activated carbon (KOH activated), cotton husk-based

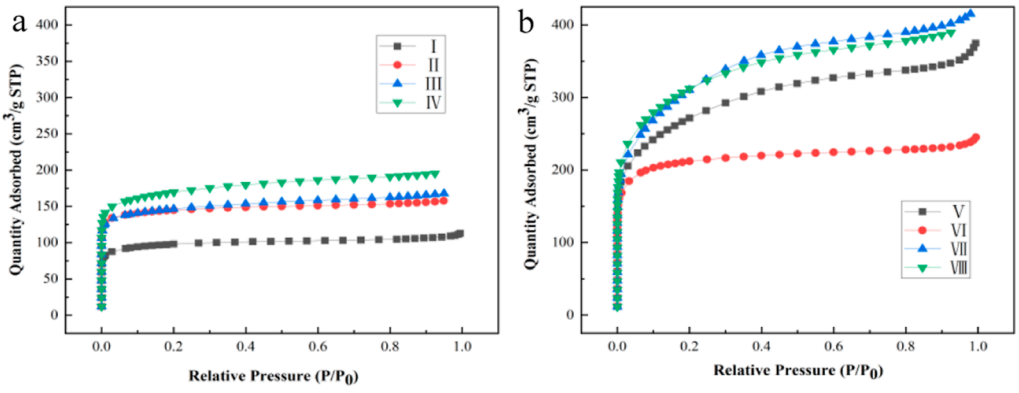

Figure 5. (a) N_2 adsorption isotherms of cotton stem-based activated carbon and (b) N_2 adsorption isotherms of cotton shell-based activated carbon.

https://doi.org/10.1021/acsomega.3c09501
ACS Omega 2024, 9, 17989−18000

Table 1. Pore Size Structure Parameters of Cotton Stem-Based Biomass Activated Carbon

sample category	specific surface area (m^2/g)	microporous area (m^2/g)	Langmuir surface area (m^2/g)	total pore volume (cm^3/g)	micropore volume (cm^3/g)	mesopore volume (cm^3/g)	average pore diameter (nm)
I	376.7019	346.6030	474.1207	0.174351	0.139221	0.035130	1.8513
II	570.6534	532.9223	687.0883	0.252277	0.208675	0.043602	1.7683
III	567.9713	494.8060	731.7873	0.269179	0.195900	0.073279	1.8957
IV	643.4680	541.1000	854.4460	0.312225	0.219563	0.092662	1.9409

Table 2. Pore Size Structure Parameters of Cotton Shell-Based Biomass Activated Carbon

sample category	specific surface area (m^2/g)	microporous area (m^2/g)	Langmuir surface area (m^2/g)	total pore volume (cm^3/g)	micropore volume (cm^3/g)	mesopore volume (cm^3/g)	average pore diameter (nm)
V	974.8847	611.8142	1500.4505	0.579739	0.269304	0.310435	2.3787
VI	815.2707	739.4945	1004.8574	0.379364	0.296927	0.082437	1.8613
VII	1106.8455	658.9340	1625.9172	0.658151	0.297934	0.360217	2.3785
VIII	1133.2194	789.8545	1713.1471	0.631742	0.342641	0.289101	2.2299

activated carbon (KOH/NaOH activated), preoxidized cotton husk-based activated carbon (KOH activation), and preoxidized cotton shell-based activated carbon (KOH/NaOH activation) were numbered as I, II, III, IV, V, VI, VII, and VIII, respectively, and the N_2 adsorption isotherms of cotton stem-based activated carbon and cottonseed hull-based activated carbon are shown in Figure 5. At 77 K, when P/P_0 was smaller than 0.1, the nitrogen adsorption isotherms increased rapidly and the adsorption capacity was strong; when $0.1 < P/P_0 < 1$, the nitrogen isotherm rises slowly and tends to equilibrium. Referring to the IUPAC classification,[3,6,7] both cotton stem-based activated carbon and the cotton shell-based activated carbon belong to the typical type I.

The specific surface areas of cotton stem-based activated carbon and cotton husk-based activated carbon and their structural parameters of pore size distribution were calculated according to the BET and Langmuir specific surface theories and are shown in Tables 1 and 2, respectively. Comparing the BET specific surface area and Langmuir surface area of KOH single activation and KOH/NaOH composite activation in Tables 1 and 2, it can be seen that there is little difference in the effect of KOH single activation and KOH/NaOH composite activation for the preparation of the cotton straw biochar, while the preoxidation treatment of the cotton stem biochar or cottonseed hull biochar was more effective. NaOH composite activation for the preparation of the cotton straw biochar did not differ much, while the preoxidation treatment of the cotton stem biochar or cottonseed hull biochar was more effective, and the average pore sizes of cotton stem-based biomass activated carbon were all lower than 2 nm, with micropores dominating, while most of the average pore sizes of cottonseed hull-based biomass activated carbon were in the range of 2−50 nm, with mesopores dominating. Considering the activation and preoxidation aspects together,[4,11,22] the specific surface area of the cotton straw biochar produced by single activation with KOH followed by preoxidation with $KMnO_4$ was more developed and there were a large number of homogeneous meso-/microporous structures, which had a higher added value.

3.1.2. SEM Characterization Analysis. The surface morphology of cotton stem-based activated carbon and cottonseed hull-based activated carbon was observed by a scanning electron microscope. Figure 6a shows the microstructure of cotton stem-based activated carbon activated by KOH/NaOH composite activation. The carbon structure is relatively loose and porous, showing a large number of fragments, and a flocculent structure is formed on the surface of the porous carbon; Figure 6b shows the microstructure of KOH single activated cotton stem-based activated carbon, with small pores and obvious tube bundle structures; Figure 6c,d, respectively, shows the microstructure of KOH/NaOH composite activated cotton stem-based activated carbon and KOH single activated cotton stem-based activated carbon after preoxidation. From the SEM diagram, it can be seen that a relatively developed pore structure appears in the cotton stem-based biochar sample activated after preoxidation, indicating that preoxidation has a better pore-forming effect on the activated biochar.

Figure 6e,f shows the microstructures of KOH single activated cottonseed hull-based activated carbon and KOH/NaOH composite activated cottonseed hull-based activated carbon, respectively. The surface of activated cottonseed hull-based powder shows a smooth ripple shape, with many pore-like structures in the cross-section; Figure 6g,h shows the microstructure of KOH single activated cotton shell-based activated carbon and KOH/NaOH composite activated cotton shell-based activated carbon after preoxidation, respectively. From the SEM diagram, it can be seen that some aggregates are also distributed on the surface of cottonseed hull-based biochar samples activated after preoxidation, with many holes and smooth and flat holes. This structure is conducive to adsorption and is a high-quality biochar adsorption material.

3.1.3. Analysis of Trace Elements in Activated Carbon. In this experiment, a 1 cm cotton stem straw was used as the precursor. Cotton stem-based activated carbon (KOH/NaOH activation), cotton stem-based activated carbon (KOH activation), preoxidized cotton stem-based activated carbon (KOH/NaOH activation), and preoxidized cotton stem-based activated carbon (KOH activation) were subjected to ICP−MS elemental analysis. After a suitable digestion method was selected, the K, Na, Ca, Mg, Cr, Cd, and Pb elements in the sample were tested by inductively coupled ion mass spectrometry; the test results are shown in Table 3. Using the same method, ICP−MS elemental analysis was performed on cottonseed hull-based activated carbon (KOH activation), cottonseed hull-based activated carbon (KOH/NaOH activation), preoxidized cottonseed hull-based activated carbon (KOH activation), and preoxidized cottonseed hull-based activated carbon (KOH/NaOH activation). The test results are shown in Table 4, with the same numbering as that above.

During the growth process of crops, trace elements such as K, Na, Ca, Mg, and Fe, which are environmentally friendly in the soil, are absorbed. From Tables 3 and 4, it can be seen that cottonseed hulls are more enriched with trace elements, such as

https://doi.org/10.1021/acsomega.3c09501
ACS Omega 2024, 9, 17989−18000

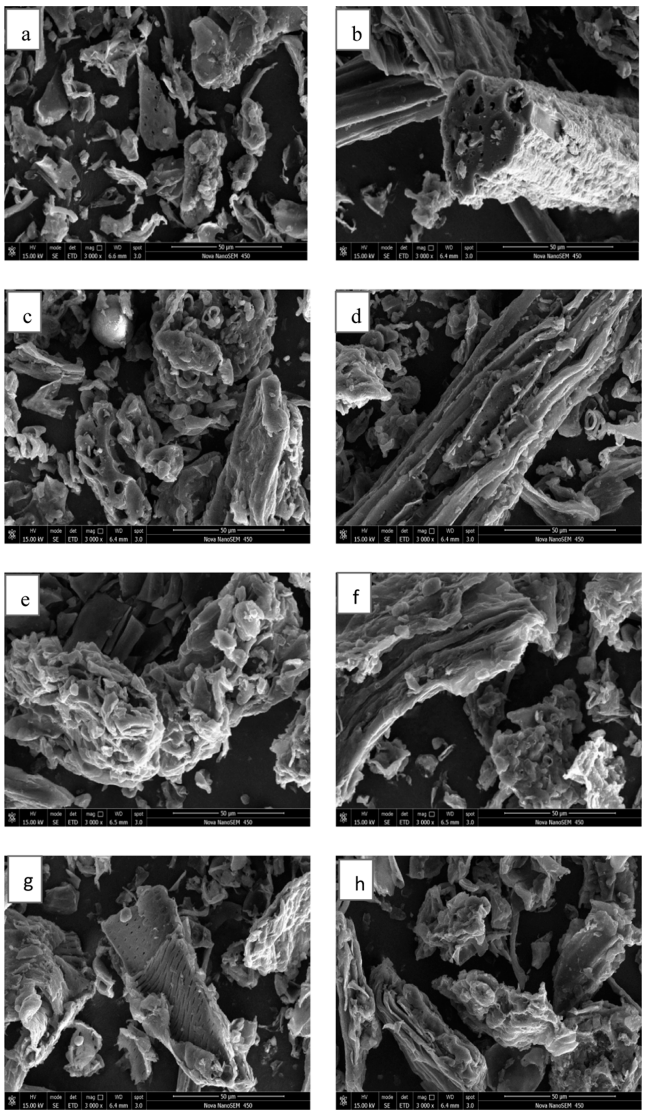

Figure 6. Scanning electron microscopy of activated carbon: (a) cotton stem-based activated carbon (KOH/NaOH activated); (b) cotton stem-based activated carbon (KOH activated); (c) preoxidized cotton stem-based activated carbon (KOH/NaOH activated); (d) preoxidized cotton stem-based activated carbon (KOH activated); (e) cotton husk-based activated carbon (KOH activated); (f) cotton husk-based activated carbon (KOH/NaOH activated); (g) preoxidized cotton husk-based activated carbon (KOH activation); and (h) preoxidized cotton shell-based activated carbon (KOH/NaOH activation).

K, Na, Ca, and Mg, than cotton stalks. After pyrolysis and carbonization of the biomass from cotton stalks and cottonseed hull, these elements are then present in the form of ash in the biomass carbonization material. Especially, the content of the Ca element is relatively high, which mainly comes from soil minerals and organic matter, and is easily absorbed by plants.

The soil in the Kashi region in China is heavily polluted by Cd, followed by Pb and Cr.[3,4] Under such circumstances, ordinary cotton plants can show strong tolerance and grow normally.[4] From Tables 3 and 4, it can be seen that cottonseed hull and cottonseed hull-based activated carbon have stronger enrichment capacity for heavy metals like Cd, Pb, and Cr than cotton stems.

3.1.4. Infrared Spectral Analysis of Activated Carbon. The infrared spectra of the cotton stem raw material (CS-I), cotton stem-based carbonization material (CSCM-I), and cotton stem-based activated carbon with different pretreatment methods are shown in Figure 7. The infrared spectra of cottonseed hull raw material (CS-II), cottonseed hull-based carbonization material (CSCM-II), and cottonseed hull-based activated carbon with different pretreatment methods are shown in Figure 8. There are obvious absorption peaks at 3430 and 3230 cm^{-1}, belonging to the stretching vibration of sugars O−H (alcohols, phenols, and carboxylic acids) and N−H. The absorption peak at 1620 cm^{-1} is caused by the stretching vibration of the olefin and benzene ring skeleton C═C; while the absorption peak at 1030 cm^{-1} is caused by the stretching vibration of C−OH and the stretching vibration of ether C−O−C, which is a characteristic peak of polysaccharides. The absorption peak at 633 cm^{-1} is caused by the angular vibration of O−H. By comparing the six curves in Figures 7 and 8, respectively, it can be seen that the vibration of the absorption peak of the biochar after alkali leaching or preoxidation is weakened, and the absorption peak at 3230 and 1315 cm^{-1} disappears, indicating that high-temperature activation and chemical modification have destroyed the organic structure in the carbonized material.[4,31−33] In summary, cotton stem-based and cottonseed hull-based activated carbon materials may mainly have the following functional groups: alcohol (phenol) hydroxyl, amino, carbon double bonds, ether bonds, and so forth; while alcohol(phenyl)hydroxyl and amino groups are hydrophilic groups, which are beneficial to adsorption.

3.1.5. Adsorption Selectivity Analysis. As is well known, biomass activated carbon has a high adsorption effect on low-concentration metal ion wastewater (0−200 mg/L), and some studies had compared biological adsorbents based on their adsorption capacity. Through comparison in Table 5, it was found that cotton straw biomass-activated carbon materials have good selectivity in adsorbing heavy metal ions.

3.2. Research on the Adsorption Performance of Activated Carbon Materials for Cd^{2+}. *3.2.1. Experimental Study on the Adsorption Performance of Activated Carbon Materials with Different Chemical Modifications for Cd^{2+}.* Preparation of the adsorption solution: about 0.1 g of CS-I, CSCM-I, I, II, III, IV, CS-II, CSCM-II, V, VI, VII, VIII, and other 12 kinds of samples were weighed, three each, and kept in 36

Table 3. Trace Elements of Cotton Stem-Based Biomass Activated Carbon

type content	K/μg/L	Na/μg/L	Ca/μg/L	Mg/μg/L	Cr/μg/L	Cd/μg/L	Pb/μg/L
blank	0.34	1.43	3.08	0.27	334	2.61	6.94
precursor	21.062	3.222	14.841	3.932	0	0	0.002
I	1.209	1.05	18.618	9.413	0	0.045	0.187
II	2.98	0.71	2.9439	8.378	0	0.043	0.864
III	2.563	1.571	38.121	6.953	0	0.089	0.508
IV	0.561	0.579	8.451	4.647	0	0.076	1.22

https://doi.org/10.1021/acsomega.3c09501
ACS Omega 2024, 9, 17989−18000

Table 4. Trace Elements of Cotton Shell-Based Biomass Activated Carbon

type content	K/μg/L	Na/μg/L	Ca/μg/L	Mg/μg/L	Cr/μg/L	Cd/μg/L	Pb/μg/L
blank	0.34	1.43	3.08	0.27	334	2.61	6.94
precursor	39.4	31.9	12.9	36.5	31.5	0.11	14.8
V	37.2	34	12.5	30.3	38.8	0.077	12.5
VI	14.7	12.4	61.9	12	32.9	0.069	12.2
VII	30.8	26.5	10.3	23.8	48.4	0.094	15.3
VIII	27	22.4	11.7	21.9	33.3	0.07	12.3

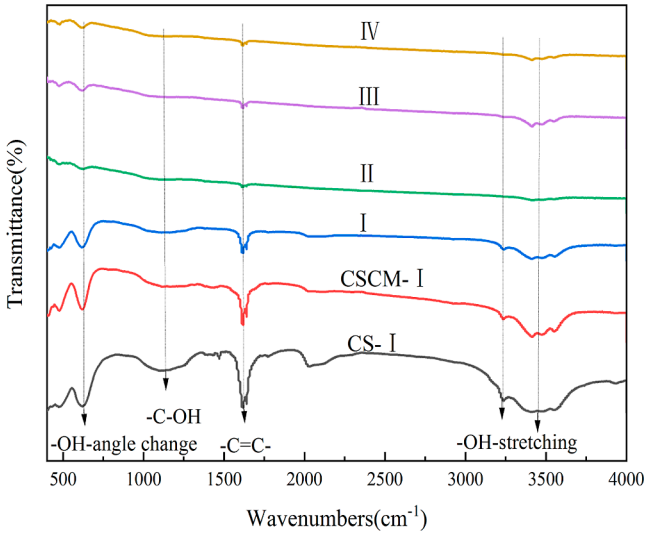

Figure 7. FT-IR spectra of cotton stem raw materials, carbonized materials, and activated carbon with different pretreatment methods.

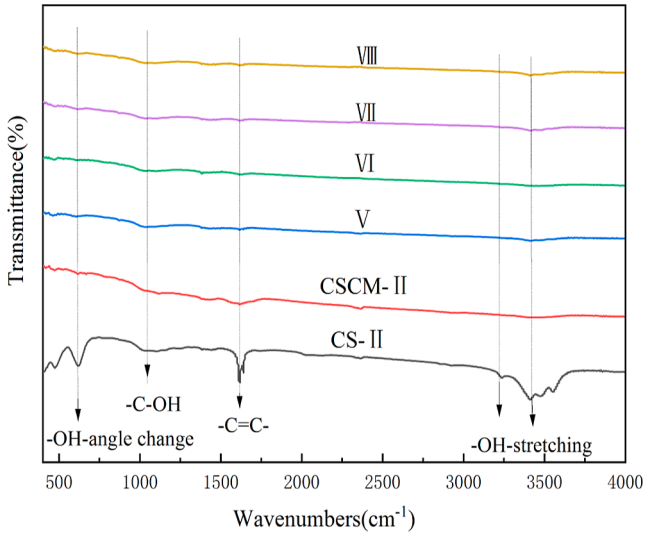

Figure 8. FT-IR spectra of cotton shell raw materials, carbonized materials, and activated carbon with different pretreatment methods.

corresponding 250 mL conical flasks. 100 mg/L of Cd^{2+} simulated wastewater solution was added, respectively. The pH was adjusted to 8 with a dilute solution of 0.2% NaOH and HNO_3, oscillated at a constant temperature of 313 K for 3 h, and then passed through a 0.45 μm membrane filter, and the experiments were repeated 5 times.

Determination of the adsorption capacity: this experiment directly used Cd^{2+} standard solution and 250 mL of cadmium ion standard sample solution was prepared with 0.2% nitric acid at 0, 0.50, 1.00, 2.00, 3.00, 4.00, and 5.00 mg/L, respectively.

Table 5. Adsorption Effect of Different Feedstocks on Heavy Metal Ions in Wastewater

no.	feedstock	heavy metal ions in wastewater	adsorption capacity/(mg/g)	reference
1	magnetic biosorbent based on kapok	Pb(II)	49.00	(Daneshfozu et al., 2017)
2	cotton ball	Cu(II)	11.40	(Ozsoy et al., 2006)
3	water Hyacinth biochar	Pb(II)	24.94	(Runjuan et al., 2021)
4	cotton straw	Pb(II)	124.70	(Wang et al., 2021)

This was used to calibrate the instrument before each measurement. The correlation coefficient of the measurement values of the standard sample solution prepared in this experiment was above 0.999. Then, the mass concentration of Cd^{2+} in the sample filtrate was determined using a WFX-220A Es flame atomic absorption mass spectrometer, and the removal rate (%) and adsorption amount (mg/g) of Cd^{2+} were calculated for 12 samples, including CS-I, CSCM-I, I, II, III, IV, CS-II, CSCM-II, V, VI, VII, and VIII. Taking the removal rate and adsorption capacity as the vertical axis, and 12 sample materials such as CS-I, CSCM-I, I, II, III, IV, CS-II, CSCM-II, V, VI, VII, and VIII as the horizontal axis, a bar chart is drawn, as shown in Figure 9. Taking into account the removal rate and adsorption capacity of different activated carbon materials for Cd^{2+}, cotton shell-based activated carbon materials have superior adsorption effects for Cd^{2+} and are an excellent adsorption material.

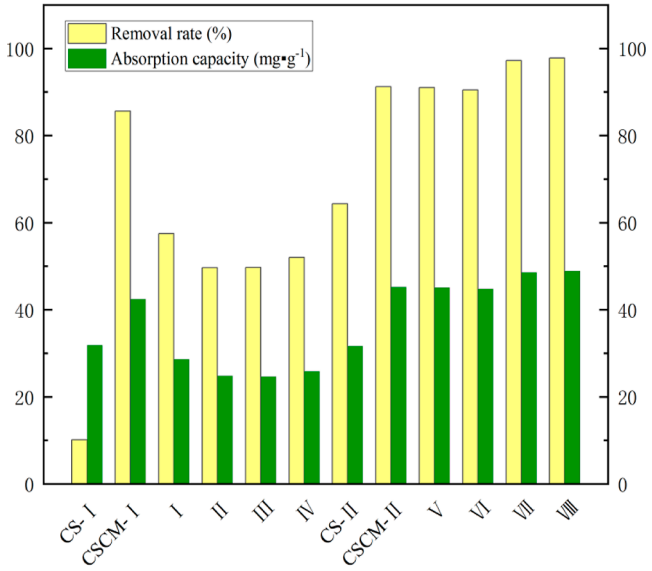

Figure 9. Adsorption effect of raw materials, carbonized materials, and activated carbon types with different pretreatment methods on Cd^{2+}.

https://doi.org/10.1021/acsomega.3c09501
ACS Omega 2024, 9, 17989−18000

Taking into account the factors of the removal rate and absorption capacity of activated carbon materials, the activated carbon numbered VIII is taken as the research object to explore the effects of adsorption time, temperature, pH value, and simulated Cd^{2+} wastewater concentration on its adsorption of Cd^{2+} from aqueous solutions and to explore the optimal experimental conditions.

3.2.2. Exploring the Effect of Cotton Shell-Based Activated Carbon (VIII) on the Adsorption of Cd^{2+} under Different Reaction Times. At the temperature of 313 K and the pH value of about 6, we used the analytical balance (precision: 0.0001 g) to take an appropriate amount of adsorbent (about 0.1 g) to treat 100 mL of simulated wastewater solution containing Cd^{2+} with the concentration of 100 mg/L in a 250 mL conical flask. The sample was kept in a constant-temperature oscillator, with a rotating speed of 120 rpm. Samples were taken (every 30 min) and filtered, respectively, after 60, 90, 120, 150, 180, and 210 min of reaction. A pipet was used to measure 5 mL of the filtrate in a 50 mL volumetric flask for constant volume (diluted 10 times), and then an atomic absorption mass spectrometer was used to measure the concentration of Cd^{2+} in the filtrate. Six parallel experiments were carried. The adsorption effect of reaction time on Cd^{2+} is shown in Figure 10. The adsorption rate of the

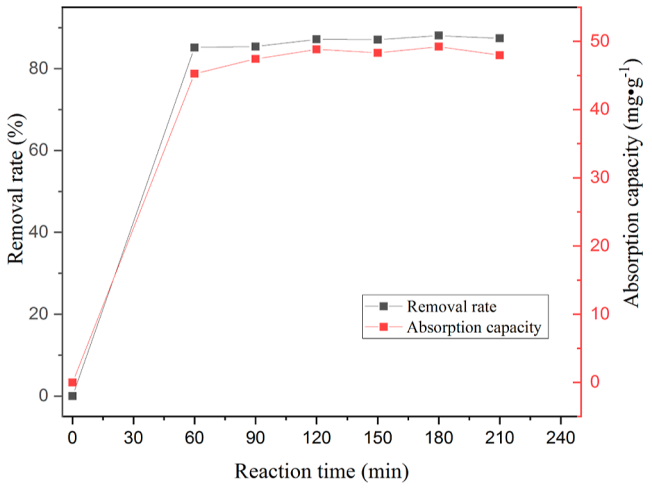

Figure 10. Effect of reaction time on the removal rate of Cd^{2+}.

adsorbent for Cd^{2+} is faster 60 min before the reaction, with an adsorption capacity of 45.25 mg/g and a removal rate of 85.16%, with a relative error within 0.05%. As the reaction time increases, the adsorption rate of the adsorbent for Cd^{2+} gradually slows until reaching the adsorption equilibrium. The adsorption equilibrium time is 180 min, and the optimal reaction time for subsequent adsorption experiments is 180 min.

3.2.3. Exploring the Effect of Cotton Shell-Based Activated Carbon (VIII) on the Adsorption of Cd^{2+} at Different Reaction Temperatures. About 0.10 g of the adsorbent was weighed under the condition of the pH value of about 6, vibrated at a constant temperature of 303, 308, 313, 318, 323, and 328 K, respectively, controlled other conditions unchanged, adopted the best reaction time, reached the adsorption equilibrium in 100 mL of Cd^{2+} simulated wastewater with a concentration of 100 mg/L, filtered with a 0.45 μm filter membrane, diluted the filtrate 10 times with the same method, measured the concentration of Cd^{2+} in the filtrate with an atomic absorption mass spectrometer, and conducted six parallel experiments. The adsorption effect of the reaction temperature on Cd^{2+} is shown in Figure 11. Before the temperature reached 318 K, as the temperature increased, the adsorption rate of the adsorbent on

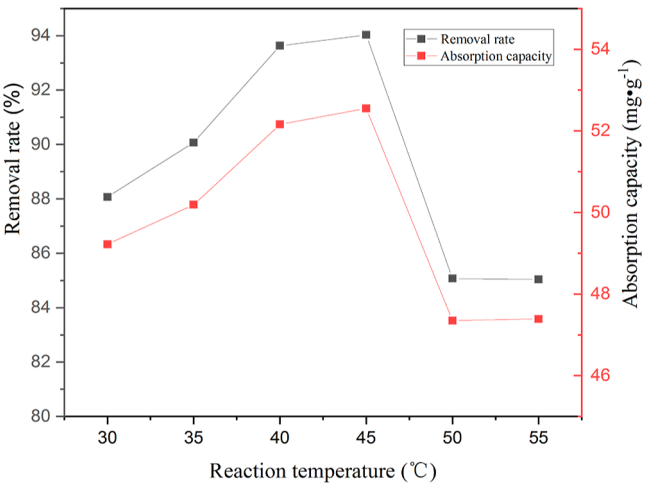

Figure 11. Effect of temperature on the removal rate of Cd^{2+}.

Cd^{2+} gradually accelerates. When the temperature is greater than 318 K, the adsorption rate of the adsorbent on Cd^{2+} rapidly decreases. At 318 K, the adsorption effect of the adsorbent on Cd^{2+} is better, with an adsorption capacity of 52.55 mg/g and a removal rate of 94.03% with the relative error within 0.05%. Taking into account the reaction temperature, 318 K is chosen as the optimal temperature.

3.2.4. Exploring the Effect of Cotton Shell-Based Activated Carbon (VIII) on the Adsorption of Cd^{2+} under Different Reaction pH Conditions. Approximately 0.10 g of the adsorbent was weighed at the optimal reaction time and temperature and 100 mL of simulated wastewater solution was adsorbed and treated with a cadmium ion concentration of 100 mg/L at pH values of 2, 3, 4, 5, 6, 7, 8, and 9. After reaching the reaction equilibrium in a constant-temperature shaker (at a speed of 120 rpm), it was filter with a 0.45 μm membrane, the filtrate was diluted 10 times using the same method, and the concentration of Cd^{2+} in the filtrate was measured using an atomic absorption mass spectrometer. Experiments were repeated independently five times. The adsorption effect of pH on Cd^{2+} is shown in Figure 12. When the pH value is between 3 and 8, the removal

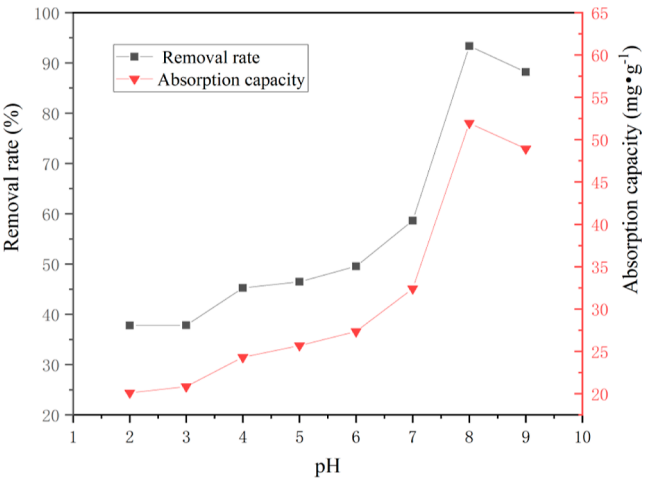

Figure 12. Effect of pH on the removal rate of Cd^{2+}.

https://doi.org/10.1021/acsomega.3c09501
ACS Omega 2024, 9, 17989−18000

rate of Cd^{2+} gradually increases from 37.77 to 93.34%, and the adsorption capacity of Cd^{2+} gradually increases from 20.11 to 51.95 mg/g with the relative error within 0.05%. The adsorption effect of Cd^{2+} gradually increases with the increase of the pH value, because at a low pH value, the surface charge of the adsorbent is positive, which is the same as the charge property of Cd (II), and the same kind of charge is mutually exclusive, The trend of Cd(II) migration to the surface of the adsorbent is relatively small.[7−12,15] As the pH value increases, the negative charge on the surface of the adsorbent increases, and positively charged Cd(II) ions are attracted by the negative charge on the surface of activated carbon. At the same time, there may also be H^+-specific adsorption sites on the carbon surface, which can exchange ions with Cd(II) cations in the solution. When the pH is greater than 8, the concentration of OH^- in the solution gradually increases, and Cd^{2+} combines with OH^- to form the $Cd(OH)_2$ precipitate. The $Cd(OH)_2$ precipitate occupies the adsorption site of the adsorbent, hindering the adsorption of Cd^{2+}. Therefore, the optimal pH value for the adsorbent to adsorb Cd^{2+} is 8.

3.2.5. Exploring the Effect of Cotton Shell-Based Activated Carbon (VIII) on the Adsorption Efficiency of Different Concentrations of Cd^{2+} in Simulated Wastewater. Approximately 0.10 g of the adsorbent was weighed and injected into wastewater with initial concentrations of 20, 40, 60, 80, 100, and 120 mg/L of Cd^{2+}. Under optimal temperature and pH conditions, the adsorption equilibrium was reacted in an air bath constant-temperature shaker (120 rpm), the mixture was filtered with a filter membrane and diluted 10 times, and the concentration of Cd^{2+} in the filtrate was measured using an atomic absorption mass spectrometer. Parallel experiments were conducted 6 times.

The adsorption effect of the initial concentration on Cd^{2+} is shown in Figure 13. When the initial concentration of Cd^{2+}

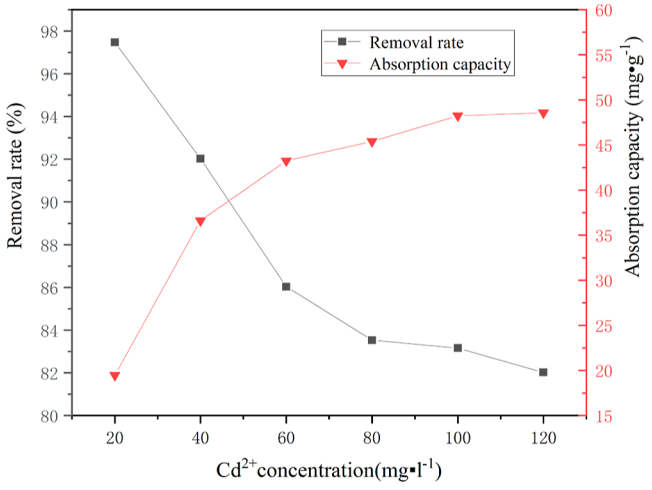

Figure 13. Effect of initial concentration on the removal rate of Cd^{2+}.

wastewater is low, the removal rate of Cd^{2+} wastewater is higher, while the adsorption capacity is lower. This is because the biological adsorption sites do not reach the saturation state at low metal concentrations. As the initial concentration increases, the biological adsorption sites gradually become saturated with the increase of metal concentration, and the removal rate of Cd^{2+} wastewater gradually decreases, while the adsorption capacity gradually increases. This experiment used approximately 0.1 g of cotton shell-based activated carbon to treat Cd^{2+} wastewater with an initial concentration of 100 mg/L, with a removal rate of approximately 84%, and an adsorption capacity of approximately 48 mg/g with the relative error within 0.05%. The adsorption effect was relatively ideal.

3.3. Adsorption Model and Fitting Analysis. *3.3.1. Analysis of Adsorption Kinetics Model Fitting.* This experiment used a quasi-first-order kinetic model and a quasi-second-order kinetic model to fit the adsorption of Cd^{2+} on cotton shell-based activated carbon (VIII). The quasi-first-order and quasi-second-order kinetic equations are detailed in eqs 3 and 4, respectively. The fitting results of the two kinetic models are shown in Figures 14 and 15, respectively

$$\lg(q_e - q_t) = \lg q_e - \frac{k_1}{2.303}t \tag{3}$$

$$\frac{t}{q_t} = \frac{1}{k_2 q_e^2} + \frac{t}{q_e} \tag{4}$$

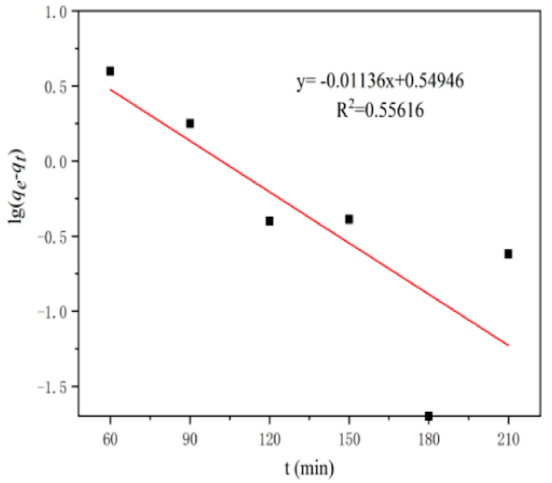

Figure 14. Pseudo-first-order model curve.

In the equation, K_1 is the adsorption reaction rate constant of the quasi-first-order kinetic model; K_2 is the adsorption reaction rate constant of the quasi-second-order kinetic model; q_t is the adsorption capacity of the adsorbent at time t (mg/g), q_e is the

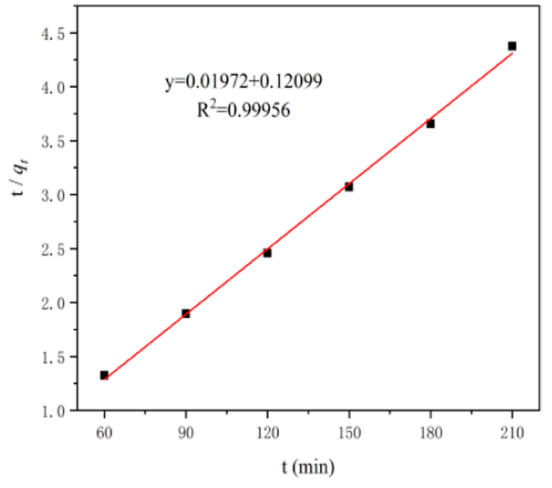

Figure 15. Pseudo-second-order model curve.

https://doi.org/10.1021/acsomega.3c09501
ACS Omega 2024, 9, 17989−18000

adsorption equilibrium capacity (mg/g), and t is the adsorption time (min).

It can be seen from Figures 14, 15, and Table 6 that by comparing and analyzing the pseudo-first-order kinetic equation

Table 6. Fitting Parameters of the Model

dynamical model	K_1	K_2	q_e	R^2	q_{max}
pseudo-first-order model	0.026162		3.5448	0.55616	49.2220
pseudo-second-order model		0.0032141	50.709	0.99956	49.2220

curves and pseudo-second-order kinetic equation curves, the pseudo-second-order kinetic model fits the reaction process of adsorption of Cd^{2+} on cotton shell-based activated carbon (VIII) more closely, with a correlation coefficient R^2 of 0.99956. The fitted value of q_e is close to the experimental value. The pseudo-second-order equation can approximate the static adsorption process of Cd^{2+} on cotton shell-based activated carbon (VIII), indicating that the pseudo-second-order kinetic model includes adsorption processes such as external liquid film diffusion, adsorption, and internal particle diffusion, which can more accurately reflect the adsorption mechanism.

3.3.2. Adsorption Isotherm Model Fitting Analysis. The adsorption process includes two processes: the adsorption of pollutants by the adsorbent and the desorption of pollutants from the adsorbent. When the adsorption rate is equal to the desorption rate, the adsorption is in dynamic equilibrium. This experiment used the Langmuir model and Freundlich model to fit the adsorption isotherm behavior. The isotherm adsorption fitting curve and related parameters are shown in Figures 16, 17, and Table 6.

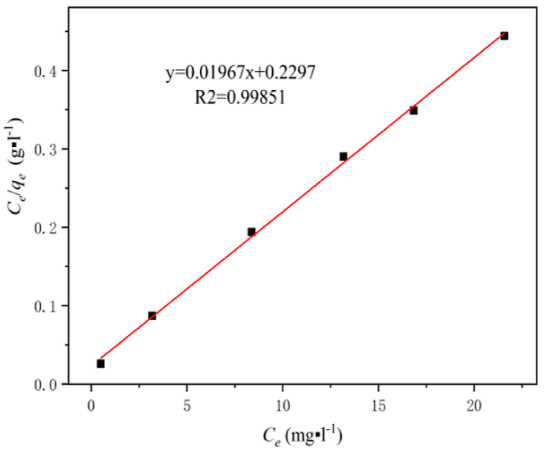

Figure 16. Fitted line of the Langmuir model.

The Langmuir model assumes that adsorption is limited to monolayer adsorption, where all adsorption sites on the adsorbent are uniformly adsorbed and have the same adsorption capacity.[12−14] The Langmuir isotherm equations are calculated using Formulas 5 and 6

$$\frac{C_e}{q_e} = \frac{C_e}{q_m} + \frac{1}{q_m b} \tag{5}$$

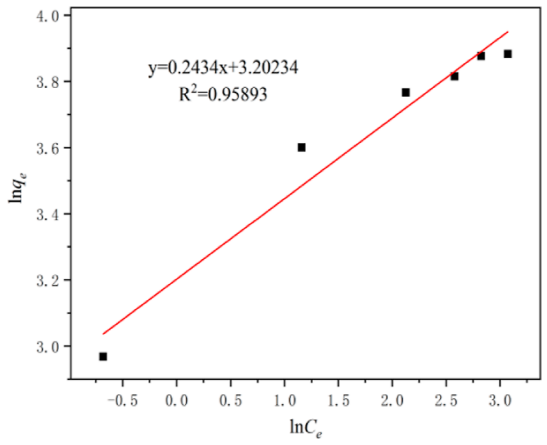

Figure 17. Fitted line of the Freundlich model.

$$R_L = \frac{1}{1 + bC_0} \tag{6}$$

In the equations, q_e is the equilibrium adsorption capacity, mg/g; q_m is the maximum adsorption capacity, mg/g; C_e is the equilibrium concentration of Cd^{2+} in the solution, mg/L; b is the Langmuir constant related to adsorption capacity and adsorption performance, L/mg; C_0 is the initial concentration of Cd^{2+}, mg/L; and the R_L dimensionless separation factor can be used to evaluate the feasibility of adsorbent adsorption using the R_L method.

The Freundlich model assumes that it is based on heterogeneous multilayer adsorption, and the adsorption contour line# temperature and related subject equation is eq 7

$$\ln q_e = \frac{1}{n}\ln C_e + \ln K_f \tag{7}$$

In the equation, K_f (mg/g) is a constant related to adsorption performance, and the slope $(1/n)$ value reflects the adsorption strength or surface heterogeneity.

In the process of Langmuir model fitting analysis, the R_L value of cotton shell-based activated carbon (VIII) adsorbed Cd^{2+} was 0.08869−0.36865, which belonged to the preferential adsorption type, and the adsorption equilibrium constant b was greater than 0, so the reaction process of adsorbent adsorption of Cd^{2+} under the experimental conditions was spontaneous; the size of k_f and n in the Freundlich isotherm adsorption model can reflect whether the adsorbent has high adsorption capacity. The larger the k_f value, the stronger the adsorbent's adsorption capacity.[7,16−19] The n value is related to the distribution of bonded ions on the surface of the adsorbent, with a value of 4.1085, ranging from 1 to 10. This also confirms that the adsorption experiment belongs to preferential adsorption and cotton shell-based activated carbon (VIII) has a strong ability to adsorb Cd^{2+}.

From Figures 16, 17, and Table 7, it can be seen that the Langmuir adsorption isotherm model performs better than the Freundlich isotherm model in the adsorption process of Cd^{2+} on cotton shell-based activated carbon (VIII), with a fitting

Table 7. Fitting Parameters of Isotherm Models

Langmuir model			Freundlich model		
b	q_m	R^2	K_f	n	R^2
0.08563	50.84	0.99851	24.59	4.1085	0.95893

https://doi.org/10.1021/acsomega.3c09501
ACS Omega 2024, 9, 17989−18000

coefficient R^2 of 0.99851, indicating a good correlation. According to the Langmuir adsorption isotherm model hypothesis,[8,20,21] it can be concluded that the adsorption process of Cd^{2+} on cotton shell-based activated carbon (VIII) is monolayer adsorption, and the surface properties of the adsorbent are relatively uniform and stable.

3.3.3. Adsorption Thermodynamic Analysis. Adsorption thermodynamics can reflect the reaction direction and degree of the reaction during the adsorption process. According to the Gibbs equation, we can calculate the ΔH, ΔS, and ΔG during the adsorption of Cd^{2+} on cotton shell-based activated carbon (VIII). Then, we analyze the effect of the temperature on the reaction. The relevant fitting curves and parameters are shown in Figure 18 and Table 8. The relevant equations are as follows

$$K_d = \frac{q_e}{C_e} \tag{8}$$

$$\Delta G = -RT\ln K_d \tag{9}$$

$$\Delta G = \Delta H - T\Delta S \tag{10}$$

$$\ln K_d = \frac{\Delta S}{R} - \frac{\Delta H}{RT} \tag{11}$$

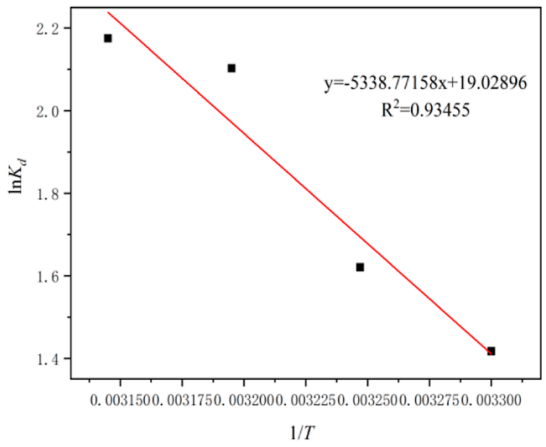

Figure 18. Relation curve between $1/T$ and ln K_d.

Table 8. Thermodynamic Parameters

T/K	ΔG/kJ/mol	ΔH/kJ/mol	ΔS/J/mol/K
303	−3.5470	44.39	158.2068
308	−4.3377		
313	−5.1287		
318	−5.9198		

In the equations, K_d is the partition coefficient; ΔG is the Gibbs free energy of the adsorption process, kJ/mol; ΔH is the enthalpy change of the adsorption process, kJ/mol; ΔS is the entropy change of the adsorption process, J/mol/K; and R is the molar gas constant, 8.314 J/mol/K.

From Table 8, it can be seen that the Gibbs free energy decreases with the increase in temperature, which is conducive to the forward progress of the adsorption process. The negative value of the Gibbs free energy also reflects the spontaneity and feasibility of the adsorption process; ΔH is +44.39 kJ/mol, which also verifies that the reaction process of cotton shell-based activated carbon (VIII) adsorption of Cd^{2+} is an endothermic reaction. If ΔS is greater than 0, it also indicates that the adsorption reaction process is an entropy-increase process, and the disorder at the solid−liquid interface increases correspondingly during the adsorption of cadmium ions by the adsorbent.[22−25]

4. CONCLUSIONS

1 This study uses cotton straw as raw material to prepare activated carbon. The BET specific surface area of cotton shell-based activated carbon is about twice that of cotton stem-based activated carbon, with well-developed pores and micropores. The BET specific surface area of cotton-shell-based activated carbon is as high as 1133.2 m^2/g, which has a high added value. From the SEM image, it can be seen that there are some aggregates and many pores distributed on the surface of cotton shell-based activated carbon, which is conducive to adsorption. Through ICP−MS elemental analysis, it was found that cotton shell-based activated carbon has a strong enrichment ability for heavy metals Cd, Pb, and Cr. FT-IR analysis found that cotton shell-based activated carbon materials mainly contain functional groups such as alcohol(phenolic)-hydroxyl groups, amino groups, carbon double bonds, ether bonds, and so forth.

2 Under the conditions of pH = 8, initial concentration of 100 mg/L, the adsorption reaction time of 180 min, adsorption temperature of 318 K, and dosage of cottonseed hull-based biomass activated carbon of about 0.1 g, the removal rate of Cd^{2+} by the adsorbent reached 94.03%, and the adsorption amount reached 51.95 mg/g, indicating a good adsorption effect.

3 The adsorption kinetic model curve conforms to the quasi-secondary kinetic model with an R^2 of 0.999; the adsorption isotherm model curve conforms to the Langmuir adsorption isotherm model with an R^2 of 0.998; and the negative Gibbs free energy of the adsorption thermodynamic fitting process reflects the spontaneity and feasibility of the adsorption process.

4 Cotton straw material has a high adsorption effect on heavy metal ions in wastewater (Table 5). With the increasing scarcity of water resources, heavy metal pollution in water bodies is becoming increasingly serious. In the current era of strict environmental protection, water treatment has become a major hotspot. In heavy metal wastewater treatment technology, cotton straw biological adsorption may become a very promising method for heavy metal wastewater treatment.

AUTHOR INFORMATION

Corresponding Author

Jing Wang − *Xinjiang Biological Solid Waste Recycling Engineering Technology Research Center, College of Chemistry and Environmental Sciences, Kashi University, Kashi 844000, China*; Email: 1085703298@qq.com

Authors

Nuremanguli Tuersun − *Xinjiang Biological Solid Waste Recycling Engineering Technology Research Center, College of Chemistry and Environmental Sciences, Kashi University, Kashi 844000, China*

Yingjie Wang − *Xinjiang Key Laboratory of Novel Functional Materials Chemistry, College of Chemistry and Environmental*

https://doi.org/10.1021/acsomega.3c09501
ACS Omega 2024, 9, 17989−18000

Sciences, Kashi University, Kashi 844000, PR China; orcid.org/0009-0007-6390-7549

Aikelaimu Aihemaiti − *Laboratory of Environmental Sciences and Technology, Xinjiang Technical Institute of Physics & Chemistry, and Key Laboratory of Functional Materials and Devices for Special Environments, Chinese Academy of Sciences, Urumqi 830011, China*

Chuanjing Huang − *Department of Chemistry, College of Chemistry and Chemical Engineering, Xiamen University, Fujian 361000, China*

Complete contact information is available at: https://pubs.acs.org/10.1021/acsomega.3c09501

Author Contributions

N.T.: data curation, visualization, formal analysis, and writing original draft. Y.W.: data curation and investigation. A.A.: writing—review and editing. J.W.: resources and writing—review and editing. C.H.: funding acquisition, methodology, project administration, resources, validation, and writing—review and editing.

Notes

The authors declare no competing financial interest.

■ ACKNOWLEDGMENTS

This research was supported by the project "Preparation and Structural Analysis of High-Performance Activated Carbon by Preoxidation of Cotton Straw in Southern Xinjiang" (2021D01B06). We want to thank the editor and anonymous reviewers for their valuable comments and suggestions for this paper.

■ REFERENCES

(1) Zuo, H. F.; Liu, Z. G. Research Progress in Preparation, Application and Modification of Sugarcane Bagasse Activated Carbon (in chinese). *Contemp. Chem. Ind.* **2023**, *52* (02), 442−446.

(2) Jiang, J. C.; Sun, K. Review on Preparation Technology of Activated Carbon and Its Application (in chinese). *Chem. Ind. For. Prod.* **2017**, *37* (01), 1−13.

(3) Chen, X.; Gu, L.; Nu, R.; Ma, C. Y.; Yang, C. Y.; Liu, X. Preparation and Characterization of Activated Carbon from Cotton Straw of South Xinjiang by KOH and KOH/NaOH Activation Method (in chinese). *J. Henan Sci. Technol.* **2015**, *559* (05), 91−95.

(4) Li, Y. W.; Mo, Z. X.; Xue, J. P. Assessment and Source Analysis of Heavy Metal Pollution in Soil of Kashi Prefecture (in chinese). *J. Arid Land Resour. Environ.* **2020**, *34* (08), 147−153.

(5) Bradshaw, A. Restoration of mined lands-using natural processes. *Ecol. Eng.* **1997**, *8*, 225−269.

(6) Daneshfozoun, S.; Abdullah, M. A.; Abdullah, B. Preparation and characterization of magnetic biosorbent based on oil palm empty fruit bunch fibers, cellulose and Ceiba pentandra for heavy metal ions removal. *Ind. Crops Prod.* **2017**, *105*, 93−103.

(7) Zak, S. Treatment of the processing wastewaters containing heavy metals with the method based on flotation. *Ecol. Chem. Eng.* **2012**, *19* (3), 433−438.

(8) Ozsoy, H. D.; Kumbur, H. Adsorption of Cu(II) ions on cotton boll. *J. Hazard. Mater.* **2006**, *136* (3), 911−916.

(9) Tan, I. A. W.; Ahmad, A. L.; Hameed, B. H. Adsorption of basic dye on high-surface area activated carbon prepared from coconut husk: Equilibrium, kinetic and thermodynamic studies. *J. Hazard. Mater.* **2008**, *154* (1−3), 337−346.

(10) Pathania, D.; Sharma, S.; Singh, P. Removal of methylene blue by adsorption onto activated carbon developed from Ficus carica bast. *Arab. J. Chem.* **2017**, *10* (1), S1445−S1451.

(11) Kannan, N.; Sundaram, M. M. Kinetics and mechanism of removal of methylene blue by adsorption on various carbons—a comparative study. *Dyes Pigm.* **2001**, *51* (1), 25−40.

(12) Purkayastha, D.; Mishra, U.; Biswas, S. A comprehensive review on Cd(II) removal from aqueous solution. *J. Water Proc. Eng.* **2014**, *2*, 105−128.

(13) Kang, S. Y.; Lee, J. U.; Moon, S. H.; Kim, K. W. Competitive adsorption characteristics of Co^{2+}, Ni^{2+}, and Cr^{3+} by IRN-77 cation exchange resin in synthesized wastewater. *Chemosphere* **2004**, *56* (2), 141−147.

(14) Alyuz, B.; Veli, S. Kinetics and equilibrium studies for the removal of nickel and zinc from aqueous solutions by ion exchange resins. *J. Hazard. Mater.* **2009**, *167* (1−3), 482−488.

(15) Rangel-Mendez, J. R.; Streat, M. Adsorption of cadmium by activated carbon cloth: influence of surface oxidation and solution pH. *Water Res.* **2002**, *36* (5), 1244−1252.

(16) Attia, A. A.; Rashwan, W. E.; Khedr, S. A. Capacity of activated carbon in the removal of acid dyes subsequent to its thermal treatment. *Dyes Pigments* **2006**, *69* (3), 128−136.

(17) Rivera-Utrilla, J.; Bautista-Toledo, I.; Ferro-García, M.; Moreno-Castilla, C. Bioadsorption of Pb(II), Cd(II) and Cr(VI) on activated carbon from aqueous solutions. *Carbon* **2003**, *41* (2), 323−330.

(18) Hansen, H. K.; Ottosen, L. M.; Kliem, B. K.; Villumsen, A. Electrodialytic remediation of soils polluted with Cu, Cr, Hg, Pb and Zn. *J. Chem. Technol. Biotechnol.* **1997**, *70* (1), 67−73.

(19) Rahman, M. S.; Islam, M. R. Effects of pH on isotherms modeling for Cu (II) ions adsorption using maple wood sawdust. *Chem. Eng. J.* **2009**, *149* (1−3), 273−280.

(20) Yao, C.; Liu, M.; Li, W. M. Adsorption capability of methylene blue by attapulgite/zinc oxide nanocomposites (in chinese). *Acta Sci. Circumstantiae* **2010**, *30* (06), 1211−1219.

(21) Qiao, Z. M.; Qin, L. L. Preparation of activated carbon from cotton shell waste by microwave irradiation and its adsorption performance (in chinese). *Chem. Eng.* **2021**, *49* (03), 6−11.

(22) Zhou, R. J.; Zhang, M.; Li, J.; Zhao, W. Optimization of preparation conditions for biochar derived from water hyacinth by using response surface methodology(RSM) and its application in pb^{2+} removal. *J. Environ. Chem. Eng.* **2020**, *8*, 104198.

(23) Gao, L. Y.; Deng, J. H.; Huang, G. F.; Li, K.; Cai, K. Z.; Liu, Y.; Huang, F. Relative distribution of Cd^{2+} adsorption mechanisms on biochars derived from rice straw and sewage sludge. *Bioresour. Technol.* **2019**, *272*, 114−122.

(24) Kulumkan, S.; Emil, O.; Gulnara, K. Activated carbon obtained from the cotton precessing wastes. *Diam. Relat. Mater.* **2019**, *91*, 90−97.

(25) Ao, W. Y.; Fu, J.; Mao, X.; Kang, Q.; Ran, C.; Liu, Y.; Zhang, H.; Gao, Z.; Li, J.; Liu, G.; et al. Microwave assisted preparation of activated carbon from biomass: A review. *Renew. Sustain. Energy Rev.* **2018**, *92*, 958−979.

(26) Zhang, X.; Liu, Z.; Cai, L.; Zhang, X.; Long, C.; Li, J.; Li, J.; Gao, Q. Development of a strong and conductive soy protein adhesive by building a hybrid structure based on multifunctional wood composite materials. *J. Clean. Prod.* **2023**, *412*, 137461.

(27) Wang, Z. Z.; Xu, J.; Yellezuome, D.; Liu, R. Effects of cotton straw-derived biochar under different pyrolysis conditions on Pb (II) adsorption properties in aqueous solutions. *J. Anal. Appl. Pyrolysis* **2021**, *157*, 105214.

(28) Zhu, Y. Q.; Zhong, M. T.; Li, W. D.; Qiu, Y.; Wang, H.; Lv, X. Cotton straw biochar and Bacillus compound biofertilizer decreased Cd migration in alkaline soil: Insights from relationship between soil key metabolites and key bacteria. *Ecotoxicol. Environ. Saf.* **2022**, *232*, 113293.

(29) Doondani, P.; Gomase, V.; Saravanan, D.; Jugade, R. Chitosan coated cotton-straw-biochar as an admirable adsorbent for reactive red dye. *Results Eng.* **2022**, *15*, 100515.

(30) Ahmed, W.; Mehmood, S.; Mahmood, M.; Ali, S.; Shakoor, A.; Núñez-Delgado, A.; Asghar, R. M. A.; Zhao, H.; Liu, W.; Li, W. Adsorption of Pb(II) from wastewater using a red mud modified rice-straw biochar: Influencing factors and reusability. *Environ. Pollut.* **2023**, *326*, 121405.

(31) Lu, H.; Zhang, W.; Wang, S.; Zhuang, L.; Yang, Y.; Qiu, R. Characterization of sewage sludge-derived biochars from different feedstocks and pyrolysis temperatures. *J. Anal. Appl. Pyrolysis* **2013**, *102*, 137−143.
(32) Zhang, L.; Tsui, T. H.; Wah Tong, Y.; Sharon, S.; Shoseyov, O.; Liu, R. Biochar applications in microbial fermentation processes for producing non-methane products: Current status and future prospects. *Bioresour. Technol.* **2023**, *386*, 129478.
(33) Zhao, Y. L.; Chen, W. Z.; Liu, F.; Zhao, P. Hydrothermal pretreatment of cotton textile wastes: Biofuel characteristics and biochar electrocatalytic performance. *Fuel* **2022**, *316*, 123327.
(34) Xia, M.; Shao, X.; Sun, Z.; Xu, Z. Conversion of cotton textile wastes into porous carbons by chemical activation with $ZnCl_2$, H_3PO_4, and $FeCl_3$. *Environ. Sci. Pollut. Res. Int.* **2020**, *27* (20), 25186−25196.
(35) Lu, L.; Fan, W.; Meng, X.; Xue, L.; Ge, S.; Wang, C.; Foong, S. Y.; Tan, C. S.; Sonne, C.; Aghbashlo, M.; et al. Current recycling strategies and high-value utilization of waste cotton. *Sci. Total Environ.* **2023**, *856*, 158798.
(36) Liew, R. K.; Azwar, E.; Yek, P. N. Y.; Lim, X. Y.; Cheng, C. K.; Ng, J. H.; Jusoh, A.; Lam, W. H.; Ibrahim, M. D.; Ma, N. L.; et al. Microwave pyrolysis with KOH/NaOH mixture activation: A new approach to produce micro-mesoporous activated carbon for textile dye adsorption. *Bioresour. Technol.* **2018**, *266*, 1−10.

https://doi.org/10.1021/acsomega.3c09501
ACS Omega 2024, 9, 17989−18000